香港中文大學
The Chinese University of Hong Kong

MAEG5160: Design for Additive Manufacturing

Lecture 12: Extensions and Applications – continue - 3

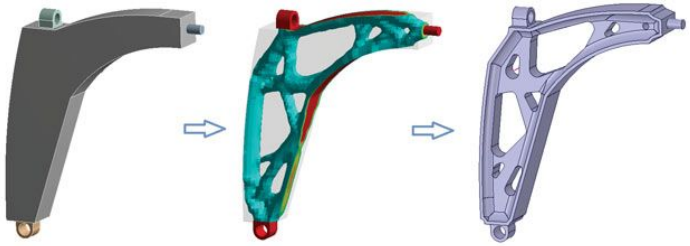

Prof SONG Xu

Department of Mechanical and Automation Engineering,
The Chinese University of Hong Kong.

Lecture 12: Extensions and Applications – continue - 3

11. Wave propagation problems

An interesting new application of the topology optimization method is the design of structures and materials subject to wave propagation. The waves may be elastic, acoustic or electromagnetic, and the phenomenon to be exploited is that for some frequency bands it is possible to construct periodic structures or materials that hinder propagation. This is called a band gap.

The phenomenon of band gaps in structures subject to periodic loads is illustrated in (a) and (b). Here a two dimensional square domain is subjected to a periodic loading at the left edge and it has absorbing boundary conditions along all four edges. The frequency of excitation of the structure in (a) is lower than for (b). It is seen that waves propagate through the structures from left to right and that the absorbing boundary conditions damp the waves at the top and bottom. These are perfectly normal situations and could model surface waves on water, acoustic waves through air, out-of plane waves in an elastic structure, polarized electromagnetic waves, etc. Now, if we introduce a periodic distribution of inclusions with different propagation speeds than in the original structures, the situation changes. For the structure subjected to the lower excitation frequency (c) , there is still propagation although the waves have different shapes. However, for the structure subjected to a higher excitation frequency (d) there seems to be no propagation at all. This illustrates the band gap phenomenon. A band gap material is defined as a material that does not allow wave propagation for certain frequency ranges. For elastic and acoustic waves the materials are called phononic band gap materials, for electromagnetic wave propagation the materials are called photonic band gap materials and the same principle on the atomic scale lies behind semiconductors. The length scale of the periodic structure in band gap materials is typically close to the wavelengths of the forbidden frequencies.

Lecture 12: Extensions and Applications – continue - 3

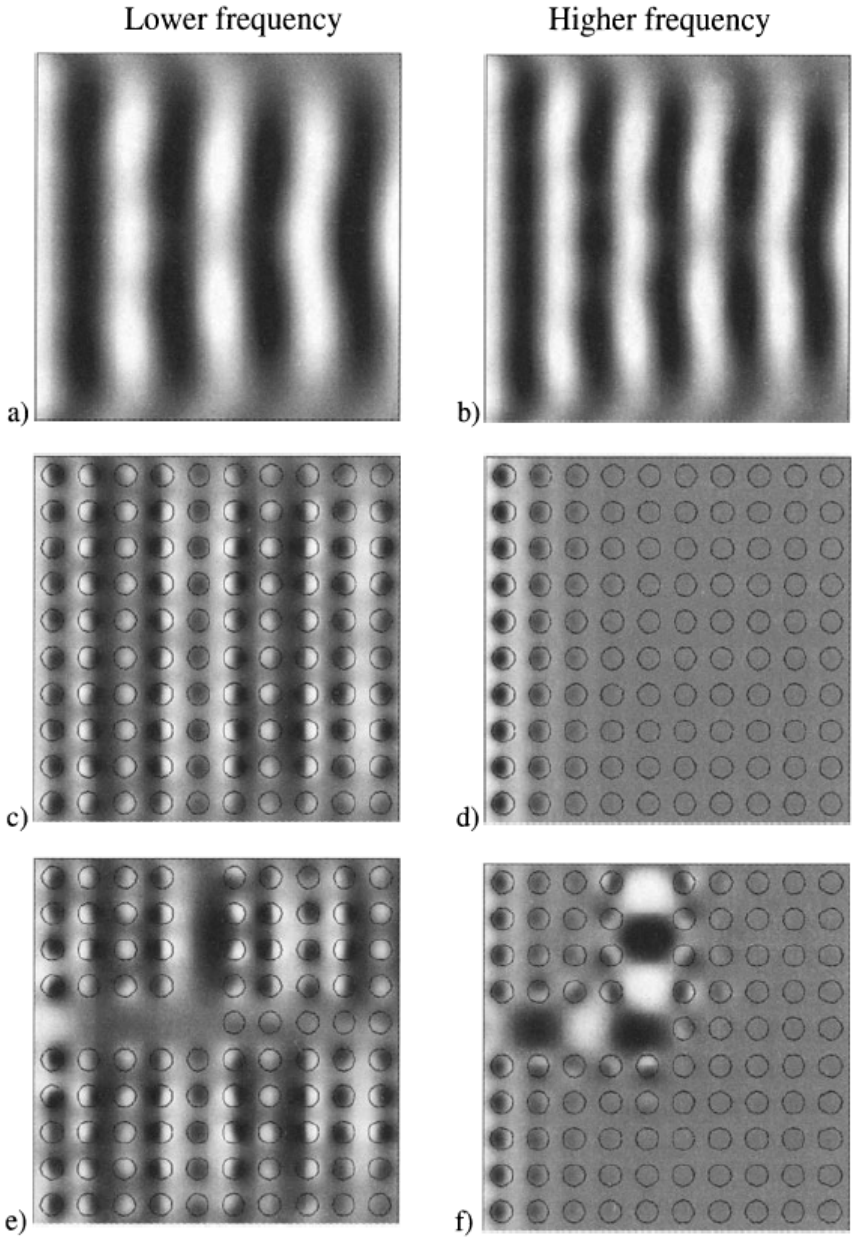

Scalar wave propagation in 2D domains with absorbing boundary conditions and forced vibrations at the left edge. a) Wave propagation through homogeneous structure, b) wave propagation with higher frequency through homogeneous structure, c) wave propagation through structure with periodic inclusions, d) (no) wave propagation with higher frequency through periodic structure, e) wave propagation through periodic structure with defect and f) wave guiding at higher frequency through a periodic structure with defect .

Lecture 12: Extensions and Applications – continue - 3

Band gap materials may be used for many purposes, for example for waveguides. The idea is illustrated in (e) and (f). If we introduce a defect in the periodic structures from (c) and (d), waves with frequencies outside the band gap may still propagate through the whole structure (e) but waves with frequencies within the band gap may now only propagate through the defect, resulting in a wave guide as seen in (f). It is seen that it is actually possible to guide waves around a corner. This is especially interesting for light waves since it may allow for the manufacturing and design of so-called photonics based microchips which have much higher clock frequencies than conventional microchips based on electrical conduction.

Apart from semiconductors and wave guides, band gap materials may be used to generate frequency filters with control of pass or stop bands, as beam splitters, as sound or vibration protection devices, as perfect mirrors and in many other applications.

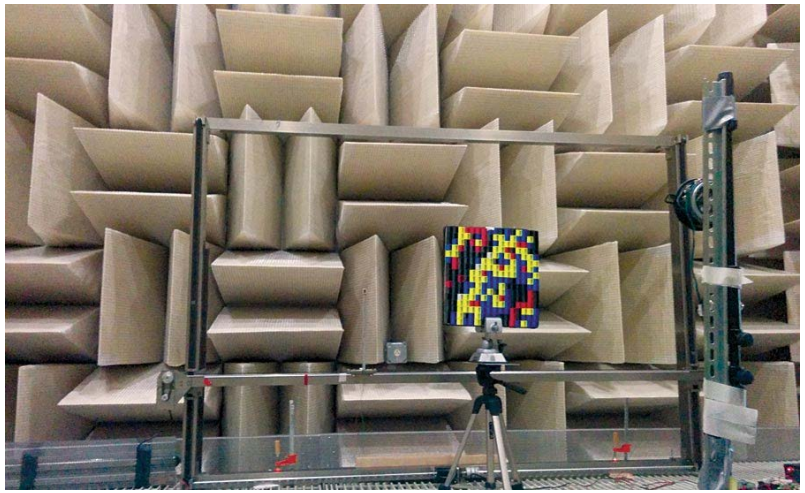

Lecture 12: Extensions and Applications – continue - 3

11.1 Modelling of wave propagation

Elastic wave propagation in a homogeneous material is governed by the Navier vector equation

$$(\lambda + \mu)\nabla(\nabla \cdot \mathbf{u}) + \mu\nabla^2\mathbf{u} - \tilde{\rho}\ddot{\mathbf{u}} = \mathbf{0} \ ,$$

where λ and μ are Lamé's coefficients, $\tilde{\rho}$ is material mass density and $\mathbf{u}$ is the point wise (vectorial) displacement.

For planar problems, the Navier equation may be split into an in-plane equation (transverse and longitudinal modes) coupled to an out-of-plane equation (also called the acoustic mode)

$$\begin{aligned}(\lambda + \mu)\nabla(\nabla \cdot \mathbf{u}_T) + \mu\nabla^2\mathbf{u}_T - \tilde{\rho}\ddot{\mathbf{u}}_T &= \mathbf{0} \ , \\ \mu\nabla^2 u_3 - \tilde{\rho}\ddot{u}_3 &= 0 \ ,\end{aligned}$$

where subscripts $_T$ and $_3$ stand for transverse and out-of-plane components, respectively.

For an inhomogeneous structure, the acoustic or out-of-plane problem

$$\nabla \cdot (\mu\nabla u) - \tilde{\rho}\ddot{u} = 0 \ , \qquad (2.46)$$

Lecture 12: Extensions and Applications – continue - 3

where the subscript $_3$ has been omitted. This equation has the same form as one of the in-plane modes for electromagnetic wave propagation (Maxwell's equations), i.e.

$$\nabla \cdot \left(\frac{1}{\epsilon} \nabla \psi \right) - \frac{1}{c^2} \ddot{\psi} = 0 \ ,$$

the so-called Transverse Electric TE-polarization mode and is closely related to the equation

$$\nabla^2 \psi - \frac{\epsilon}{c^2} \ddot{\psi} = 0 \ ,$$

governing the so-called Transverse Magnetic TM-polarization mode. Here, ϵ is the electric permitivity and c is the speed of light in vacuum.

In the following, we just consider the scalar problem (2.46). The wave equation (2.46) may be solved for a structure subject to forced periodic loading or it may be solved as a cell problem assuming an infinite periodic structure.

For the structural problem we assume that the waves are harmonic and described by $u_3 = \hat{u}_3 e^{(i\Omega t)}$, where Ω is the driving frequency and $\hat{u}_3$ is the amplitude. Substituting this into (2.46) and dropping the hats we get

$$\nabla \cdot (\mu \nabla u) + \Omega^2 \tilde{\rho} u = 0 \ .$$

This equation may be written in finite element notation as

$$\left(\mathbf{K} + i\Omega \mathbf{C} - \Omega^2 \mathbf{M} \right) \mathbf{u} = \mathbf{f} \ ,$$

Lecture 12: Extensions and Applications – continue - 3

where we have added (harmonic) boundary forces $\mathbf{f}$ and a damping matrix $\mathbf{C}$ that models absorbing boundary conditions and/or structural damping. This equation has a form which is very similar to the one used for forced structural vibration (cf., Sect. 2.1.2).

For periodic structures (i.e. materials) the wave equation may also be treated as an eigenvalue problem. As for the homogenization problem (Sect. 2.10.1), we may solve the global problem by analysing the base cell Y. In contrast to usual homogenization problems, however, the modes may not be cell periodic and therefore we cannot just impose the usual periodic boundary conditions. Instead we assume that the modes can be described by the expression

$$u(\mathbf{y},\mathbf{k}) = v(\mathbf{y})e^{i\mathbf{k}^T\mathbf{y}}e^{i\omega t} \ , \tag{2.48}$$

where v is a Y-periodic displacement field, $\mathbf{y}$ is the spatial coordinate and $\mathbf{k}$ is the wave vector. For $\mathbf{k} = \mathbf{0}$, the solution mode $u(\mathbf{y})$ will be Y-periodic. For $\mathbf{k} = \boldsymbol{\pi}$, the solution mode will be 2Y-periodic. For other $\mathbf{k}$, the solution modes can take any kind of periodicity in all directions. This kind of modelling is based on the so-called Floquet-Bloch wave theory

Inserting (2.48) in (2.46) we get the eigenvalue problem

$$\left(\nabla \cdot (\mu \nabla v) + \omega^2 \tilde{\rho} v\right) e^{\mathbf{k}^T\mathbf{y}} = 0,$$

Lecture 12: Extensions and Applications – continue - 3

which in principle should be solved for any wave vector $\mathbf{k}$. However, due to symmetry we may restrict the wave vector to the first Brillouin zone $\mathbf{k} \in [-\pi, \pi]^d$ (d is the dimension) This corresponds to analysing the structural response to incident waves of any possible wave length and direction. If we furthermore assume that the base cell is square symmetric (i.e. is quadratic and symmetric around horizontal, vertical and diagonal lines), we may restrict the range of wave vectors to the triangular region indicated It is generally accepted (but to the authors knowledge, not proved) that one only has to search the borders of the triangular region to obtain a description of the band gap structure of a periodic material. This means that the wave equation (2.49) only has to be solved for a number of wave vectors along the lines $\Gamma \to X$, $X \to M$ and $M \to \Gamma$

In finite element notation (2.49) may be written as

$$\left(\mathbf{K}(\mathbf{k}) - \omega^2 \mathbf{M}\right) \mathbf{v} = \mathbf{0} \,, \qquad (2.50)$$

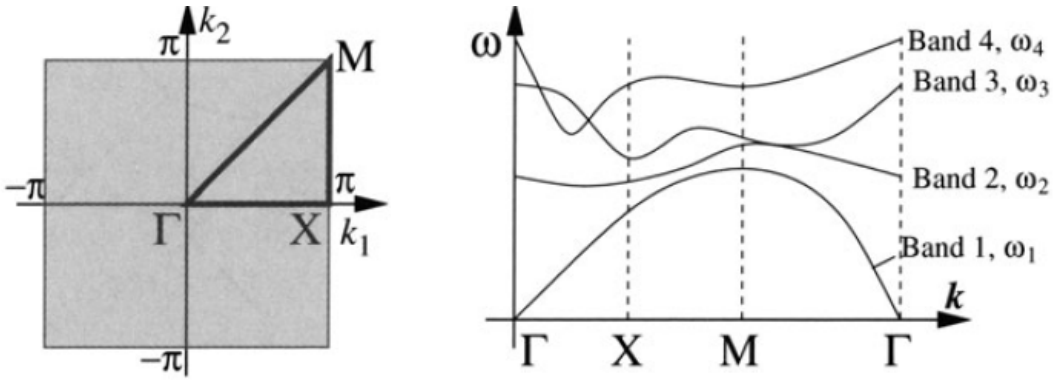

Left: The irreducible Brillouin zone indicating the wave vectors to be searched for the general 2D case (grey area). For square symmetry, the wave equation only has to be calculated for k-vector values along the curve *r* - X - *M* - *r* . Right: Sketch of band structure indicating lowest four eigenvalues for wave vectors along the line *r* - X - *M* - *r* in the irreducible Brillouin zone.

Lecture 12: Extensions and Applications – continue - 3

which is a standard eigenvalue problem. Since K is a Hermitian matrix and M is real, symmetric and positive definite, the eigenvalues of (2.50) will all be real and positive. If one solves for the first few eigenvalues of (2.50) for a number of k, the results can be plotted as a band diagram as sketched in (right). From the curves one may read the propagation modes for given frequencies.

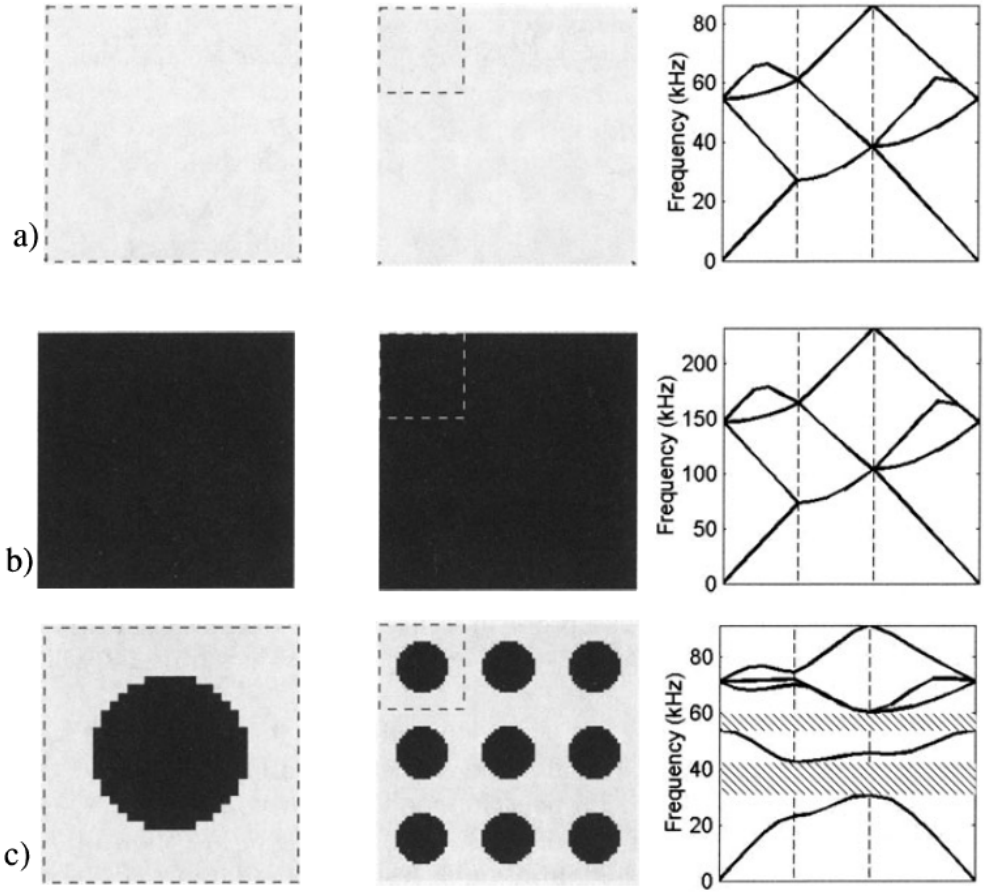

Left: single cell, middle: 3 by 3 arrays of cells and right : band structure of a) pure epoxy, b) pure duralumin and c) duralumin cylinders (radius 30% of cell size) in epoxy. Hatched areas denote band gaps. The horizontal axes denote values of the wave vector k on the boundary of the irreducible Brillouin zone. The band diagrams are based on the solution of 15 eigenvalue problems with varying k.

Lecture 12: Extensions and Applications – continue - 3

Real band diagrams for out-of-plane polarized waves are shown in (a) and (b) for pure epoxy and duralumin, respectively. It is seen that for these homogeneous materials there exist eigenmodes for any frequency, i.e. there are no band gaps. (c) shows the band structure of duralumin cylinders (radius equal to 30% of cell size) in an epoxy matrix. It is seen that there are ranges of frequencies with no corresponding eigenmodes. This means that no modes will propagate for these frequencies. There is a large band gap between the first and the second band (from 31 kHz to 43 kHz corresponding to a relative gap size of $\Delta f / fo = 0.32$) and a small gap ($\Delta f / fo = 0.11$) between the second and the third band. This means that no elastic waves with frequencies within the band gaps may propagate through the structure. The band gap zones are indicated with hatched regions in the diagram. We may now consider two kinds of optimization problems. Either we optimize the *material problem* or we optimize the *structural problem*.

11.2 Optimization of band gap materials

An obvious goal for the optimization of band gap materials is to maximize the relative band gap size. In this way the range of prohibited frequencies will be wider and more signals may be sent through a waveguide based on defects in the band gap material. The design problem is a two material problem. We want to distribute two non-void phases in the design domain (base cell). For reasons that will become clear later, we here choose a linear material interpolation between the phases, i.e. the wave shear modulus and mass density are interpolated as

Lecture 12: Extensions and Applications – continue - 3

$$\mu(\rho_e) = (1-\rho_e)\mu_1 + \rho_e\mu_2 \quad \text{and} \quad \tilde{\rho}(\rho_e) = (1-\rho_e)\tilde{\rho}_1 + \rho_e\tilde{\rho}_2 \ ,$$

where μ_1 and μ_2 are the shear moduli of material one and two, respectively, $\tilde{\rho}_1$ and $\tilde{\rho}_2$ are the mass densities, and the interpolation density ρ_e belongs to $[0,\ 1]$.

The objective is to maximize the relative band gap size between to bands j and $j+1$, i.e. maximizing the lowest value of the overlying bands and minimizing the maximum value of the underlying bands. This can be written as a (double) max-min problem

$$\max_{\boldsymbol{\rho}} \left\{ c(\boldsymbol{\rho}) = \frac{\Delta\omega^2(\boldsymbol{\rho})}{\omega_0^2(\boldsymbol{\rho})} = 2\, \frac{\min\limits_{\mathbf{k}} \omega_{j+1}^2(\mathbf{k},\boldsymbol{\rho}) - \max\limits_{\mathbf{k}} \omega_j^2(\mathbf{k},\boldsymbol{\rho})}{\min\limits_{\mathbf{k}} \omega_{j+1}^2(\mathbf{k},\boldsymbol{\rho}) + \max\limits_{\mathbf{k}} \omega_j^2(\mathbf{k},\boldsymbol{\rho})} \right\} .$$

This is a "dirty" objective function in the sense that it is a max-min problem with varying critical points (the k-vector(s) for the critical frequencies may change during the optimization) and it may have several multiple eigenvalues. Interestingly, however, there is no need for a volume fraction constraint in the problem since neither a pure phase one structure produces a band gap (a) and nor does a pure phase two structure (b). Somewhere in between there must be a volume fraction that results in the biggest band gap. Another interesting observation is that due to the missing volume constraint, the usual SIMP interpolation becomes useless in ensuring black-and-white designs. However, this is not a big problem since by experience, the optimized designs tend to be mostly black and white anyway. Finally, the mesh-independent filtering techniques works badly due to the missing volume constraint. Therefore, the regularized penalty function method is used to ensure black-and-white and mesh-independent designs for this design problem.

Lecture 12: Extensions and Applications – continue - 3

The optimization problem may then now be written as

$$\begin{aligned}
\max_{\boldsymbol{\rho}} \quad & \frac{\Delta\omega^2(\boldsymbol{\rho})}{\omega_0^2(\boldsymbol{\rho})} \\
\text{s.t.}: \quad & \left[\mathbf{K}(\mathbf{k}) - \omega^2\mathbf{M}\right]\mathbf{u} = \mathbf{0}, \quad \mathbf{k} \in [\Gamma - X - M - \Gamma] \,, \\
& 0 \leq \rho_e \leq 1, \quad e = 1, \ldots, N \,,
\end{aligned}$$

and may be rewritten in the more convenient bound formulation

$$\begin{aligned}
\max_{\boldsymbol{\rho}} \quad & = \beta \\
\text{s.t.}: \quad & \left[\omega_{j+1}(\mathbf{k})\right]_m \geq \beta, \quad m = 1, \ldots, M \,, \\
& \left[\omega_j(\mathbf{k})\right]_m \leq \beta \qquad m = 1, \ldots, M \,, \\
& \left[\mathbf{K}(\mathbf{k}) - \omega^2\mathbf{M}\right]\mathbf{u} = \mathbf{0}, \quad \mathbf{k} \in [\Gamma - X - M - \Gamma] \,, \\
& 0 \leq \rho_e \leq 1, \quad e = 1, \ldots, N,
\end{aligned}$$

where the two first constraints take the *M* most critical values into account. This problem may efficiently be solved using MMA.

Lecture 12: Extensions and Applications – continue - 3

Results from optimizing the epoxy /duraluminum structures from previous case are shown below. The first example maximizes the relative band gap size between the first and the second band. The result is an almost square inclusion of a duraluminum in the epoxy matrix. The relative band gap size has increased from 0.32 for the circular inclusion in previous (c) to 0.65 for the square inclusion structure in below (a). The second example maximizes the relative band gap size between the second and the third band. In this case, the resulting structure consists of diamond and circular inclusion of duraluminum inclusions in the epoxy matrix. The relative size of the second band gap has increased from 0.11 for the circular inclusion in previous (c) to 0.61 for the structure in (b) below.

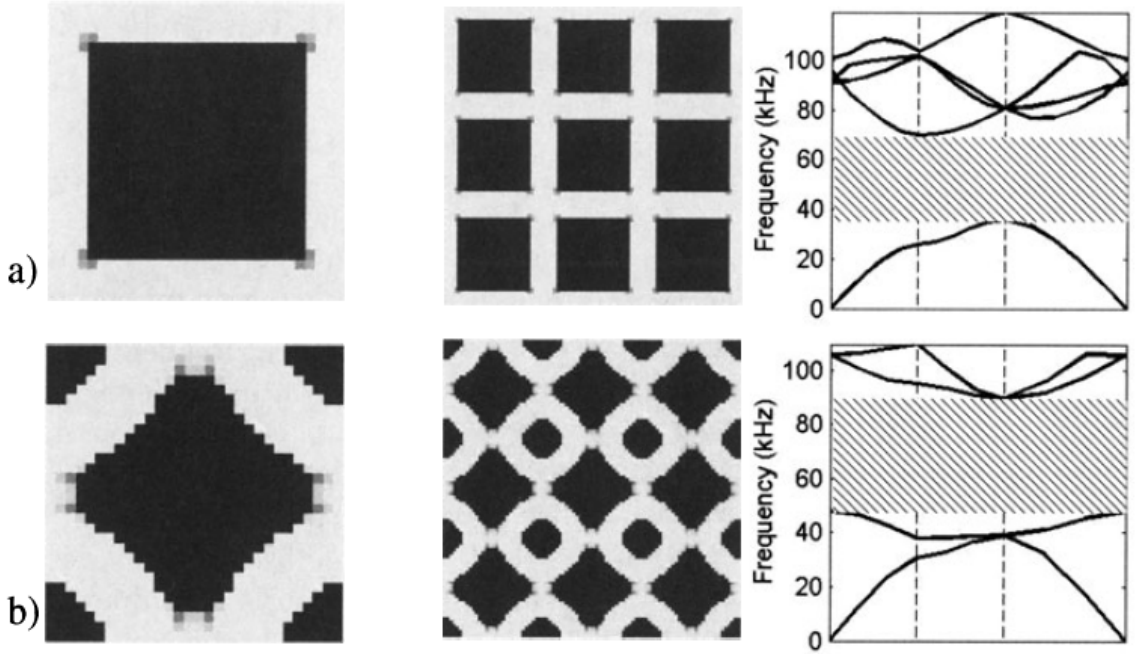

Maximization of relative band gap size between a) first and second band and b) second and third band.

Lecture 12: Extensions and Applications – continue - 3

11.3 Optimization of band gap structures

The material design problem in the previous sub-section assumed infinite periodicity of the material. This means that the influence of boundaries as well as the influence of defects in the periodic structure can not be modelled. In order to model finite domains we use the wave equation and the objective function here may be to minimize the magnitude of the wave at the boundaries (hinder wave propagation) or to maximize the wave at certain points in the structure (wave-guiding). The optimization problem looks very much like the one defined for structures subjected to forced vibrations. Here, however, the input point and the point to be damped are not coincident. The difference may be seen as the difference in optimizing for minimum compliance and in optimizing compliant mechanisms.

An optimization problem solving the problem of minimizing the wave magnitude at a point, a line or an area of a structure subjected to forced vibrations with frequency can be written as

$$
\begin{aligned}
&\min_{\boldsymbol{\rho}} \quad c = \bar{\mathbf{u}}^T \mathbf{L} \mathbf{u} \\
&\text{s.t.}: \quad (\mathbf{K} + i\ \Omega\ \mathbf{C} - \Omega^2 \mathbf{M})\ \mathbf{u} = \mathbf{f}\ , \\
&\qquad \sum_{e=1}^{N} v_e \rho_e \leq V, \qquad 0 < \rho_{min} \leq \rho_e \leq 1, \quad e = 1, \ldots, N\ ,
\end{aligned}
$$

Lecture 12: Extensions and Applications – continue - 3

where $\mathbf{L}$ is a zero matrix with ones at the diagonal elements corresponding to the degrees of freedom of the nodes, lines or areas to be damped. Due to the complex damping term, the solution of (2.47) is complex and we use overbar $(\bar{\cdot})$ for the complex conjugate. This formulation corresponds to (2.6) with an added damping term and a slightly modified objective function.

The sensitivities of the objective function can by the adjoint method be found as

$$\frac{\partial c}{\partial \rho_e} = 2\Re\left(\boldsymbol{\lambda}^T \left[\frac{\partial \mathbf{K}}{\partial \rho_e} + i\Omega\frac{\partial \mathbf{C}}{\partial \rho_e} - \Omega^2\frac{\partial \mathbf{M}}{\partial \rho_e}\right]\mathbf{u}\right) ,$$

where $\Re(\cdot)$ means real part and $\boldsymbol{\lambda}$ is the solution to the adjoint equation

$$\left(\mathbf{K} + i\mathbf{C} - \Omega^2\mathbf{M}\right)\boldsymbol{\lambda} = -\mathbf{L}\bar{\mathbf{u}} .$$

Lecture 12: Extensions and Applications – continue - 3

shows an example where the suggested optimization procedure is used to minimize wave propagation through a square plate. The left edge if subjected to forced vibrations with frequency $\Omega = 200$, the left and right edges have absorbing boundary conditions and the top and bottom edges are free. The size of the plate is 0.12, the shear moduli are $\mu_1 = 0.384$ and $\mu_2 = 0.769$ and the specific densities are $\tilde{\rho}_1 = \tilde{\rho}_2 = 1$ (all data is normalized). The objective is to minimize the average amplitude at the right edge. The resulting structure is not unexpected a grid of alternating phase one and phase two material corresponding to a Bragg grating. This structure is known to reflect one dimensional waves. Compared to un-damped wave propagation, the magnitude of the outgoing wave has been decreased by almost 3 orders of magnitude.

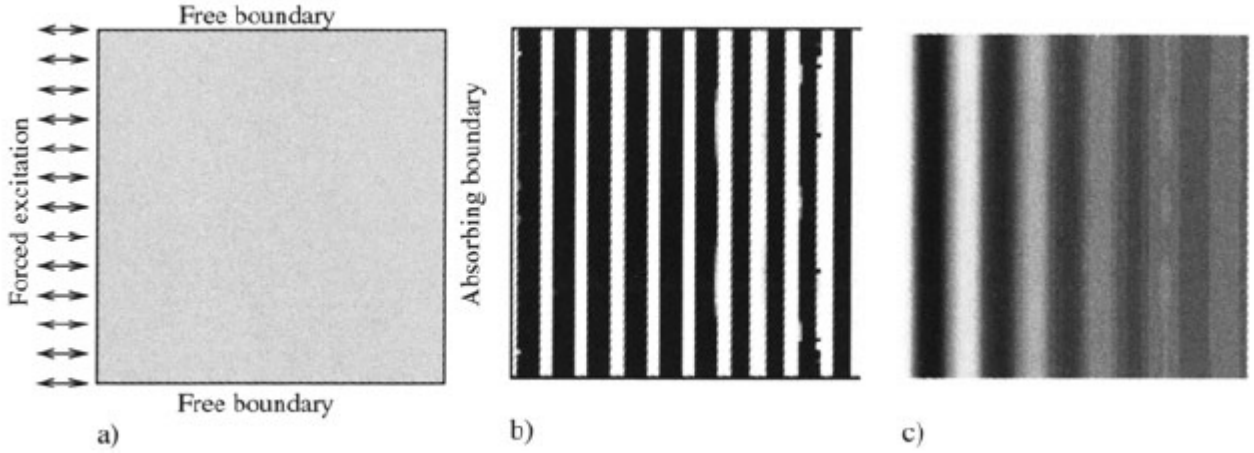

Damping of wave propagation in a quadratic plate. a) Design domain and boundary conditions, b) optimized structure and c) the wave field

Lecture 12: Extensions and Applications – continue - 3

The problem formulation may also be used to design wave guides as shown in below. Here, all edges have absorbing boundary conditions. The centerpart of the left edge is subjected to forced vibrations and the objective function is to *maximize* the wave magnitude at the center of the lower edge. The resulting structure is intriguing. Apparently, the wave is bent by a wave guide based on curved Bragg gratings. It is seen from the wave picture (c) that the mode at the output port is almost as strong as at the input port.

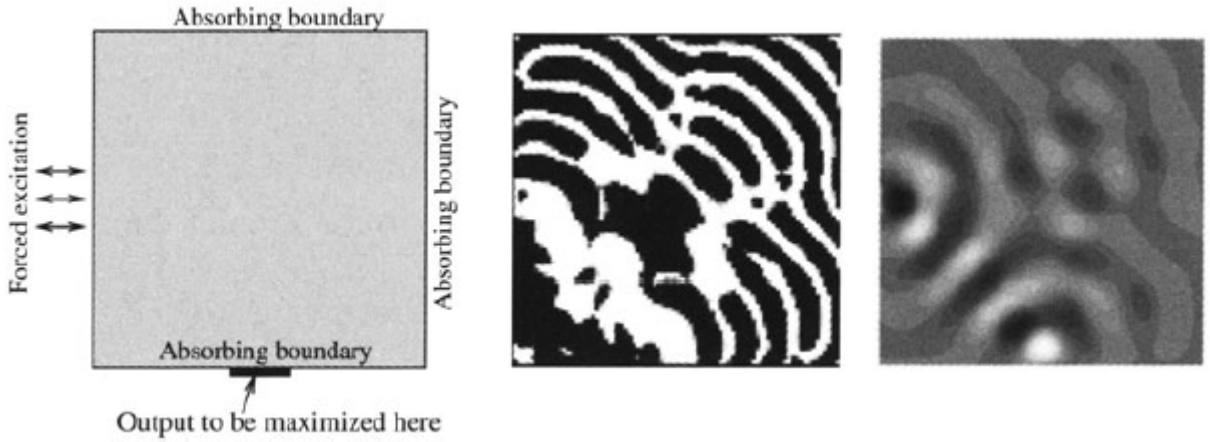

Optimization of wave guidance in a quadratic plate. a) Design domain and boundary conditions, b) optimized structure and c) the wave field

Lecture 12: Extensions and Applications – continue - 3

12 Various other applications (without mathematical details)

12.1 Material design for maximum buckling load

Previously we discussed a new class of materials with extremal elastic properties. This material class makes use of infinitely fine laminations of the constituent material phases - so-called rank-l laminates. Such materials are from a practical point of view not very useful since they have very low critical buckling loads when the softer phase has close to zero stiffness. Therefore, it makes sense to optimize material structures for buckling load rather than for normal linear loads. As we also discussed under bone-remodelling, a buckling load criterion may very well be the reason for why bone structure is a stiffness sub-optimal open-walled cell structure. In order to eliminate lamination type structures in the periodic cell, one may introduce a local buckling load constraint on the cell problem, just as we did for structural buckling problems in. However, there is no guaranty that a cell periodic buckling mode is the most critical one, and therefore we should include also non-cell periodic buckling modes when we search for the most critical buckling load. This can be done by Floquet-Bloch wave analysis for wave propagation problems. Below shows a buckling load diagram for varying wave-vectors k and some of the associated buckling modes for a specific square microstructure. It is seen that the most critical buckling mode is the shear mode which has a buckling load that is less than a third of the cell periodic mode. This demonstrates the importance of using Floquet-Bloch wave theory for modelling the problem.

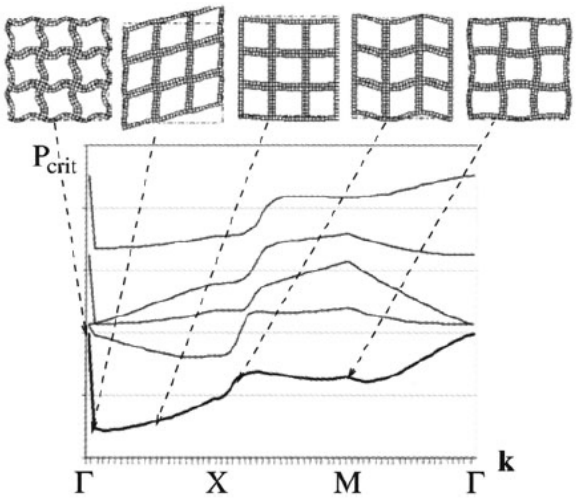

Modelling of non-local buckling using Floquet-Bloch wave theory

Lecture 12: Extensions and Applications – continue - 3

Figure below shows another example of a critical load diagram for square microstructures. The material structures are subject to uniaxial horizontal loading and we allow a total volume fraction of 0.52 to be filled with stiff material. In the first case (Fig. 2.55a), the outer square frame is fixed to be solid and the rest of the material is evenly distributed in the interior of the cell. This results in a non-dimensionalized buckling load of 0.029. Now we maximize the minimum buckling load over all wave vectors along the lines r - X - M - r in the Brillouin zone. The optimized topology and its associated buckling diagram is shown in (a). The buckling load for the optimized material structure is 0.061 - an increase of more than a factor of two.

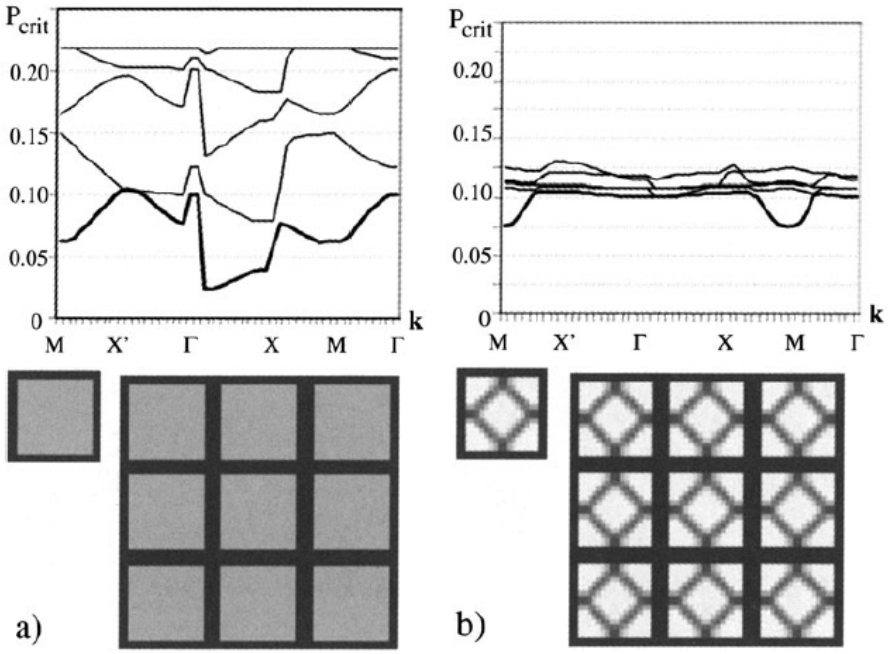

Maximization of microstructural buckling load. a) Initial design with buckling load 0.029 and b) topology optimized design with buckling load 0.061

Lecture 12: Extensions and Applications – continue - 3

12.2 Bio-mechanical simulations

Models for bone remodelling and optimal design have mutually provided inspiration for new developments in either area for a collection of papers dealing with such aspects. It thus turns out that there is a close similarity between the optimality criteria algorithm and schemes for bone remodelling. Also, in many isotropic remodelling algorithms, the relationship between density and the elasticity modulus of cancellous bone is modelled exactly like in the SIMP model. Furthermore, when orthotropy is taken into account, Wolff's law for bone predicts that stresses and material axes are aligned, exactly as for minimum compliance design. Even though it is commonly agreed that the bone does not attain, from a structural optimization point of view, a stable optimal configuration with respect to any given static loads, the similarity between the two types of modelling has suggested that optimal remodelling will provide a framework for simulating the adaptation of bone structure that is subject to external loading. We will not elaborate further on this here, but refer to the vast literature on the subject.

Bone remodelling simulation for multiple loads. Femur longitudinal cuts. Two sets of results depending on cost of bone creation

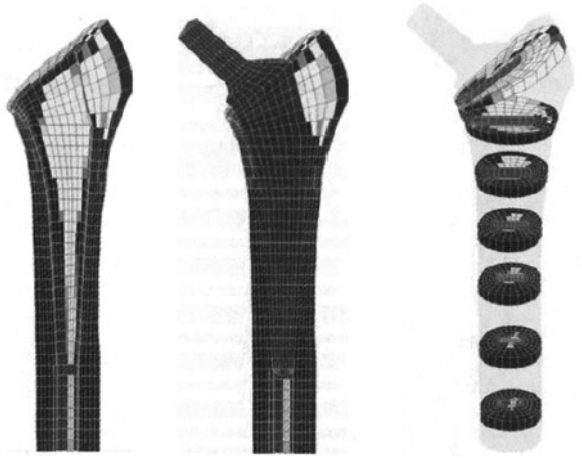

Bone remodelling with tapered hip prosthesis, contact conditions, for multiload case and with bone ingrowth modelling

Lecture 12: Extensions and Applications – continue - 3

12.3 Applications in the automotive industry

Since the introduction of the idea of treating structural topology optimization as a material distribution problem this subject has evolved substantially and it has changed the design process in the automotive industry by providing better structures, not only in the early stages of the process, but also as a technique to improve component designs in subsequent phases. Structural topology optimization is an important tool for structural designers in the automotive industry. In the first half of the 20th century, new structural designs were obtained using much of the experience of the designer. However, with the introduction of structural optimization in the early 1960s, plus the advances in topology optimization in the 1990s, design processes have changed dramatically in the industry. Nowadays, computers help to create new topological designs in a matter of minutes using commercially available structural topology optimization software. The applications of such tools in the design cycle have had a tremendous impact on the final product and in the design process as well. There are many types of structural problems that can be encountered in the automotive industry, from simple linear static problems like a bracket design, to non-linear transient problems like designing for crashworthiness.

Lecture 12: Extensions and Applications – continue - 3

12.3.1 Stiffness maximization of vehicle structures

The structural body of a vehicle is required to provide a stiffness in bending and torsional directions beyond some lower limits prescribed by the design team based on previous experiences and/or competitive vehicles. Maximization of the stiffness is equivalent to minimization of the mean compliance of the structure under a given load. This type of problem can be solved not only for components, but also for vehicle structural skeletons (body structures). In its multiload format, more than 80% of structural topology design optimization problems in industry can be addressed by solving compliance minimization problems. Here one often seeks the Pareto curve by solving several optimization problems for different sets of weights. This is a very common situation in automobile design, where two or more responses go through a trade-off analysis to determine the final design. Figure below shows a compliance optimized body structure (also known as "the body in white") of a sedan vehicle. The finite element meshes used for such structures can easily reach 200,000 or more finite elements. The design objective is to maximize the torsional and bending stiffness. These two stiffnesses are important for static loading, for ride and handling and also from the vibrational point of view.

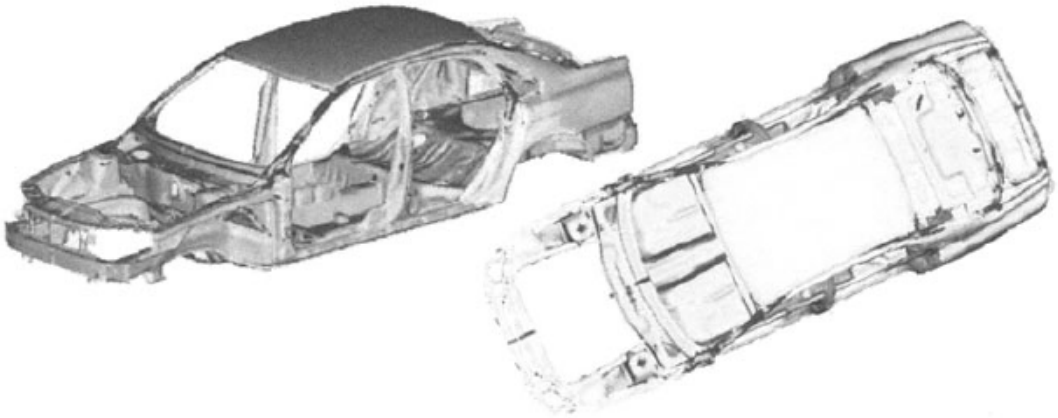

A compliance optimized body structure of a sedan vehicle. Dark areas indicate where more material improves the performance in torsional and bending stiffness simultaneously.

Lecture 12: Extensions and Applications – continue - 3

12.3.2 Noise, vibration and harshness (NVH)

NVH is a vehicle response that passengers feel and judge continuously when the car is running. Vibrations from 20 Hz up to 5000 Hz must be minimized in a vehicle design to reduce discomfort on passengers. There are three main sources of vibrations: power train (engine and transmission), wind, and road-tire interaction. Each one of them has its own frequency range and are resolved in different ways. Power train vibrations are well defined in terms of their frequency spectrum since they come at known rpm values. In such cases, the optimization problem has the design objective of preventing structural natural frequencies to coincide with the power train frequencies. Wind vibration and noise are caused by vibratory pressure of the wind on windshield, window glasses and other external panels. These vibrations are usually reduced by changes in the contour and finish of the vehicle external surfaces. Vibrations corning from road-tire interaction (harshness) are more difficult to treat because the range of frequencies is very wide and sometimes it is impossible to provide a structure with low vibration for the entire range. There are two main approaches to deal with structural vibration problems. If the frequency spectrum of loads is very well defined with distinguishable frequencies, the manipulation of the natural frequency spectrum is the better approach. Moving up or down natural frequencies can be achieved using topology optimization techniques. However, if the frequency spectrum of loads is very dense, with almost white noise characteristics, the reduction of the magnitude of vibrations is the better approach. This can be done when the simulation is performed as a forced frequency vibration problem, rather than a free (eigenvalue) vibration problem. The former approach works on the cause of the problem, while the latter works on the symptoms.

Lecture 12: Extensions and Applications – continue - 3

12.3.3 Design for stress reduction - durability

Durability is the term used to describe the fatigue phenomena in the automotive industry. The goal is to build a vehicle with a useful life span of several hundred thousands kilometers without experiencing any fatigue problems. The main difficulty lies in the prediction of life (number of loading cycles) for the random loads acting during the life time of the vehicle. Even more difficult is to compute sensitivity coefficients of life with respect to changes in the thickness of panels or changes in curvature. In addition, there has always been a controversy about including local constraints in topology optimization problems. One side of the argument is that topology is a global property of the structure and should not be subject to point-wise constraints. On the other hand, local topology features (such as holes) are often dominated by local structural behavior (e.g., stresses). Nevertheless, there has been several attempts to include local stresses into the problem formulation.

Reliability by brand for cars up to five years old

Rank	Brand	Score
1.	Lexus	98.7%
2.	Mitsubishi	97.9%
3.	Toyota	97.7%
4.	Mini	96.8%
5.	Skoda	96.4%
6.	Hyundai	96.3%
7.	Kia	95.9%
8.	Honda	95.3%
=9.	BMW	95.2%
=9	Mazda	95.2%
11.	Alfa Romeo	94.6%
=12.	Fiat	94.5%
=12.	Subaru	94.5%
=14.	Dacia	94.4%
=14.	Suzuki	94.4%
=16.	Citroën	93.8%
=16.	Volvo	93.8%
18.	Ford	93.7%
19.	Seat	93.6%
20.	Volkswagen	93.2%
21.	Jaguar	91.8%
=22.	Audi	91.5%
=22.	MG	91.5%
=22.	Porsche	91.5%
25.	Peugeot	91.1%
26.	Mercedes	91.0%
=27.	Nissan	90.1%
=27.	Vauxhall	90.1%
29.	Tesla	88.6%
30.	Renault	87.6%
31.	Land Rover	78.2%

Lecture 12: Extensions and Applications – continue - 3

12.3.4 Topology of embossed ribs in structural shells

One technique used to increase local stiffness of structural shells is the addition of embossed ribs (also knows as beading). These are stamped indentations with given length, depth and separation to provide directional rigidity to the shell. The difference between doing the standard topology optimization and embossed rib optimization is that the goal is not to look for isotropic material layout, but for a layout and orientation of a fixed orthotropic stiffness property. More specifically, when the design variable is close to zero, the local stiffness property (membrane and bending components) must be of an isotropic material plate of given thickness; and when the design variable is close to one, the local stiffness properties must be that of an orthotropic ribbed plate. In order to achieve this a new model is needed to simulate the structural behavior of embossed ribs based on orthotropic plate modelling. Since the local stiffness properties then depend on the amount and location of the embossed ribs and also depend on their orientation, the optimization problem is posed with two design variables, namely local rib-amount and orientation.

Lecture 12: Extensions and Applications – continue - 3

12.3.5 Crashworthiness

One of the most complicated optimization problem we can think of is the optimization of transport vehicles for crashworthiness. First, the modelling is extremely complicated, involving geometric and material non-linearities, contact and very complex geometries. Second, especially for automotive structures, the load conditions are unknown since a crash between two cars or a crash of a single car against a wall, a tree or a roll-over may happen in infinitely many ways. Third, the sensitivity analysis for path-dependent and dynamic problems is rather involved. These complications may be the reason why not much work has been done in applying topology optimization methods to crash worthiness design problems. Further problems that are expected in the applications of topology optimization methods to crash worthiness problems is how to model the response for intermediate density materials and internal contact. Ford Motor Company has built up an in-house software for crashworthiness design based on the RADIOSS software for modelling. The topology optimization can be categorized as a re-enforcement optimization problem and is performed based on heuristic criteria without sensitivity analysis.

BMW i8 soft-top attachment component is 3D printed with aluminum

Lecture 12: Extensions and Applications – continue - 3

A short description of recent work on topology optimization of frame structures for crashworthiness is given in the following. The work considers simplified planar models ignoring contact between elements. However, the sensitivity analysis is derived analytically which makes the algorithm very efficient. The modelling is based on plastic beam elements and an implicit dynamic Newmark time-stepping algorithm for obtaining the transient response. The formulation of the optimization problem must accommodate conflicting criteria such as a maximum acceleration constraint to avoid driver and passenger injuries due to too high g-forces (e.g. whip-lash) and a maximum deformation constraint to avoid passenger and driver injuries due to penetration of the passenger cabin. These requirements are best met by a structure with constant high acceleration (for example just below the head injury criteria (HIC) acceleration) throughout the crash. Therefore the optimization problem is formulated as a min-max problem where the error in obtaining the prescribed acceleration in *M* design points is minimized. This optimization problem may be written as

$$
\begin{aligned}
&\min_{\mathbf{h}} \max_{m=1,2\ldots,M} |\ddot{u}_m(\mathbf{h}) - \ddot{u}_m^*| \\
&\text{s.t.} : \mathbf{r}(t,\mathbf{h}) = \mathbf{0}, \\
&\sum_{e=1}^{N} h_e b_e l_e \leq V, \\
&0 < h_{min} \leq h_e \leq h_{max}, \quad e = 1,\ldots,N\ ,
\end{aligned}
$$

where b_e is the thickness of element e, l_e its length and h_e is the design variable (height of the beams). The residual $\mathbf{r}(t,\mathbf{h}) = \mathbf{0}$ describes the dynamic equilibrium where t is the time.

Lecture 12: Extensions and Applications – continue - 3

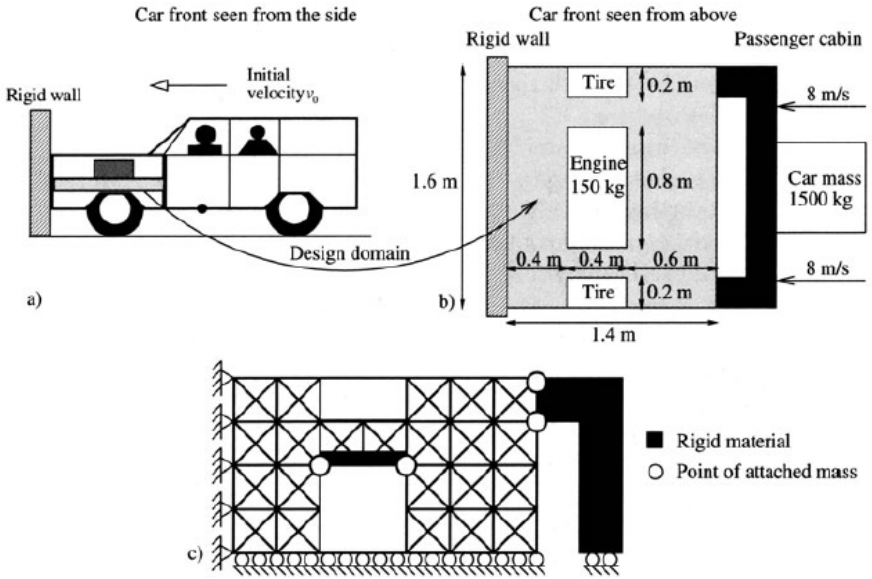

Sketch of the design domain for crashworthiness design of a car. The front part of the car is modelled by 272 plastic beam elements (c).

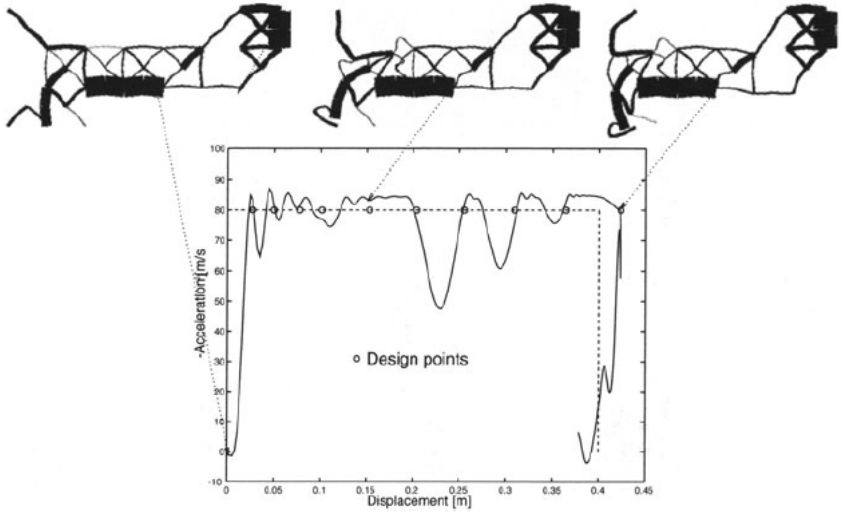

Topology optimized frame structure. Response curve and snapshots of the deformations. The goal was to obtain a constant acceleration throughout the crash.

Thank you for your attention